

Magnetic ordering effects in the phonon spectra of orthorhombic RMnO_3 compounds

This article has been downloaded from IOPscience. Please scroll down to see the full text article.

2007 J. Phys.: Condens. Matter 19 176211

(<http://iopscience.iop.org/0953-8984/19/17/176211>)

View [the table of contents for this issue](#), or go to the [journal homepage](#) for more

Download details:

IP Address: 129.252.86.83

The article was downloaded on 28/05/2010 at 17:53

Please note that [terms and conditions apply](#).

Magnetic ordering effects in the phonon spectra of orthorhombic RMnO_3 compounds

J M Wesselinowa and St Kovachev

Department of Physics, University of Sofia, Boulevard J Bouchier 5, 1164 Sofia, Bulgaria

Received 22 January 2007

Published 30 March 2007

Online at stacks.iop.org/JPhysCM/19/176211

Abstract

The phonon properties of orthorhombic manganites RMnO_3 are studied using a Green's function technique taking into account anharmonic spin–phonon and phonon–phonon interaction terms. The strong spin–phonon interaction leads to anomalies in the phonon energy and the damping around the magnetic phase transition. The phonon spectrum is discussed for different exchange interaction J_1 and spin–phonon interaction R_{sp} constants. In dependence on the sign of R_{sp} we obtain softening or hardening of the phonon modes with decreasing temperature below the phase transition temperature T_N . This is associated with phonon modulation of the exchange interaction. It is shown that the phonon energy and the phonon damping depend on the radius of the rare earth ion r_R and on the ion doping. The influence of the external magnetic field is discussed, too.

1. Introduction

The rare earth and yttrium manganites, RMnO_3 , crystallize in two structural phases: the orthorhombic structure for R with larger ionic radius ($R = \text{La, Ce, Pr, Nd, Sm, Eu, Gd, Tb}$ or Dy), while compounds with smaller ionic radius ($R = \text{Ho, Er, Tm, Yb, Lu, Y}$) can be obtained either in the orthorhombic or the hexagonal structure. A hexagonal-to-orthorhombic phase structural transition can also take place upon annealing under high pressure. The hexagonal RMnO_3 compounds belong to the class of ferroelectromagnetic materials characterized by the coexistence of magnetic and ferroelectric orderings [1]. This is not the case in the orthorhombic RMnO_3 compounds where magnetic ordering also occurs but not ferroelectric ordering. Recently Lorenz *et al* [2] have found a remarkable increase (up to 60%) of the dielectric constant with the onset of magnetic order at 42 K in the metastable orthorhombic structures of YMnO_3 and HoMnO_3 that proves the existence of strong magnetoelectric coupling in the compounds. The properties of manganites attracted significant interest since colossal magnetoresistance was observed in $\text{R}_{1-x}\text{A}_x\text{MnO}_3$ ($R = \text{rare earth or Y; A} = \text{Sr, Ca, Ba, Pb}$) [3, 4]. It was recently demonstrated that the magnetic and orbital structures in these materials depend strongly on the ionic radius r_R of the rare earth ion [5–8]. Moreover, with

decreasing r_R the low temperature antiferromagnetic (AFM) ordering changes from A-type AFM to E-type AFM [6] through an incommensurate structure. It has been shown that the magnetic ordering below T_N in LaMnO_3 [9–11] and NdMnO_3 [12] results in softening of a Raman active mode near 610 cm^{-1} , involving mainly in-plane stretching oxygen vibrations. This softening has been discussed by Granado *et al* [10] in terms of spin–phonon coupling caused by phonon modulation of the superexchange integral. It was established from Laverdiere *et al* [8] that while the materials RMnO_3 with large R^{3+} ionic radius r_R and A-type AFM order ($\text{R} = \text{Pr}, \text{Nd}, \text{Sm}$) exhibit significant phonon softening and other anomalies with decreasing temperature near and below T_N , the effect of magnetic ordering is much weaker or negligible in compounds with $\text{R} = \text{Eu}, \text{Gd}, \text{Tb}, \text{Dy}, \text{Ho}$ and Y , characterized by small r_R and incommensurate magnetic structure. But for the In- and Tl-based $\text{A}_2\text{Mn}_2\text{O}_7$ compounds, Granado *et al* [13] have observed a hardening of two of the low-energy phonons below the ferromagnetic–paramagnetic transition T_C . All Raman modes show decreasing frequencies when going from Y- to In- and Tl-based compounds. In principle, the spin–phonon interaction plays an important role in many magnetic materials [14, 15]. It renormalizes the spin-wave and the phonon spectrum. The magnetic ordering influences strongly the phonon energy and phonon damping and must be taken into account if we want to explain the experimental data.

The aim of the present paper is to study the phonon properties in magnetite compounds using a Green’s function technique beyond the random phase approximation.

2. The model

The Hamiltonian of the system can be presented as:

$$H = H_m + H_{\text{ph}} + H_{\text{sp-ph}}. \quad (1)$$

H_m is the Hamiltonian for the magnetic subsystem, which is given by the Heisenberg Hamiltonian:

$$H_m = -\frac{1}{2} \sum_{\langle ij \rangle} J_1(i, j) \mathbf{S}_i \cdot \mathbf{S}_j - \frac{1}{2} \sum_{[ij]} J_2(i, j) \mathbf{S}_i \cdot \mathbf{S}_j - g\mu_B H \sum_i S_i^z. \quad (2)$$

S_i is the Heisenberg spin at the site i , and the exchange integrals J_1 and J_2 represent the coupling between the nearest and next-nearest neighbours, respectively. H is an external magnetic field parallel to the z axis. $\langle ij \rangle$ and $[ij]$ denote the once-summation over the nearest- and the next-nearest-neighbours, respectively.

In order to investigate the phonon spectrum and the experimentally obtained strong spin–phonon coupling we have to consider the following two terms in equation (1). The second term H_{ph} contains the lattice vibrations including anharmonic phonon–phonon interactions:

$$H_{\text{ph}} = \frac{1}{2!} \sum_q (P_q P_{-q} + (\omega_q^0)^2 Q_q Q_{-q}) + \frac{1}{3!} \sum_{q, q_1} B(q, q_1) Q_q Q_{-q_1} Q_{q_1-q} + \frac{1}{4!} \sum_{q, q_1, q_2} A(q, q_1, q_2) Q_{q_1} Q_{q_2} Q_{-q-q_2} Q_{-q_1+q}, \quad (3)$$

where Q_q , P_q and ω_q^0 are the normal coordinate, momentum and frequency, respectively, of the lattice mode with a wavevector \mathbf{q} . The vibrational normal coordinate Q_q and the momentum P_q can be expressed in terms of phonon creation and annihilation operators:

$$Q_q = (2\omega_q^0)^{-1/2} (a_q + a_{-q}^\dagger), \quad P_q = i(\omega_q^0/2)^{1/2} (a_q^\dagger - a_{-q}). \quad (4)$$

$H_{\text{sp-ph}}$ describes the interaction of the magnetic spins with the phonons. This is very important in order to explain the experimental data of Raman and IR spectroscopy lines in manganites:

$$H_{\text{sp-ph}} = \sum_q \bar{F}_{\text{sp}}(q) Q_q S_{-q}^z - \frac{1}{2} \sum_{q,p} \bar{R}_{\text{sp}}(q,p) Q_q Q_{-p} S_{p-q}^z + \text{h.c.}, \quad (5)$$

where

$$\bar{F}_{\text{sp}}(q) = \frac{1}{\sqrt{N}} \sum_h \frac{1}{|h|} (e_q \cdot h) J_1'(h) \exp(iq \cdot h), \quad (6)$$

$$\bar{R}_{\text{sp}}(p,q) = \frac{1}{N} \sum_h \left(J_1''(h) - \frac{J_1'(h)}{|h|} \right) (e_{p-q} \cdot h) (\exp(ip \cdot h) + \exp(iq \cdot h)). \quad (7)$$

The summation extends over the vectors $\mathbf{h} = \mathbf{r}_i - \mathbf{r}_j$ connecting all possible pairs of spin sites in the crystal and e_q is the polarization of the phonon with wavevector \mathbf{q} . $F_{\text{sp}}(q) = \bar{F}_{\text{sp}}(q)/(2\omega_q^0)^{1/2}$ and $R_{\text{sp}}(q,p) = \bar{R}_{\text{sp}}(q,p)/(2\omega_q^0)^{1/2}(2\omega_p^0)^{1/2}$ designate the amplitudes for coupling phonons to the spin-wave excitations in first and second order, respectively.

3. The phonon Green's function

The retarded phonon Green's function to be calculated is defined as:

$$G(\mathbf{k}, \omega) = \langle\langle a_{\mathbf{k}}; a_{\mathbf{k}}^\dagger \rangle\rangle, \quad (8)$$

where $a_{\mathbf{k}}, a_{\mathbf{k}}^\dagger$ are the phonon annihilation and creation operators. For the approximate calculation of the Green's function we use a method proposed by Tserkovnikov [16], which is appropriate for spin problems. After a formal integration of the equation of motion for the Green's function one obtains

$$G_{ij}(t) = -i\theta(t) \langle [a_i; a_j^\dagger] \rangle \exp(-i\omega_{ij}(t)t) \quad (9)$$

where

$$\omega_{ij}(t) = \omega_{ij} - \frac{i}{t} \int_0^t dt' t' \left(\frac{\langle [j_i(t); j_j^\dagger(t')] \rangle}{\langle [a_i(t); a_j^\dagger(t')] \rangle} - \frac{\langle [j_i(t); a_j^\dagger(t')] \rangle \langle [a_i(t); j_j^\dagger(t')] \rangle}{\langle [a_i(t); a_j^\dagger(t')] \rangle^2} \right) \quad (10)$$

with the notation $j_i(t) = \langle [a_i, H_{\text{int}}] \rangle$. The time-independent term

$$\omega_{ij} = \frac{\langle [[a_i, H]; a_j^\dagger] \rangle}{\langle [a_i; a_j^\dagger] \rangle} \quad (11)$$

is the energy in the generalized Hartree–Fock approximation (GHFA). The time-dependent term in equation (10) includes damping effects.

The modulation of the spin-wave energy E (equation (18)) and exchange interaction constant J_1 (equation (19)) by specific zone-centre lattice vibrations is responsible for a spin–phonon coupling, manifested by a renormalization of the phonon frequencies below the magnetic ordering temperature T_N . We have calculated the phonon energy beyond the RPA and obtain the following expression which is renormalized due to the spin–phonon interaction:

$$\omega(\mathbf{k})^2 = \omega_0^2 - 2\omega_0 \left(M^2 R_{\text{sp}}(\mathbf{k}) - \frac{1}{2N} \sum_q A(\mathbf{k}, \mathbf{q}) (2\bar{N}_q + 1) - B(\mathbf{k}) \langle Q(\mathbf{k}) \rangle \delta_{k0} \right), \quad (12)$$

with

$$\langle Q(\mathbf{k}) \rangle = \frac{M^2 F_{\text{sp}}(\mathbf{k}) - \frac{1}{N} \sum_q B_{kq} (2\bar{N}_q + 1)}{\omega_0 - M^2 R_{\text{sp}}(\mathbf{k}) + \frac{1}{N} \sum_q A_{kq} (2\bar{N}_q + 1)}. \quad (13)$$

$\omega(\mathbf{k})$ contains the phonon energy ω_0 , a term due to the spin–phonon interaction (caused by the modulation of the exchange integral by lattice vibrations) and two terms due to the phonon–phonon interactions (including lattice expansion/contraction due to anharmonicity and/or magnetostriction effects). $M = \langle S^z \rangle$ is the relative magnetization and is calculated from the spin Green’s function. Above the phase transition temperature the spin–phonon interactions do not contribute to the phonon energy because M vanishes; only the anharmonic phonon–phonon interactions remain.

The phonon damping is calculated as:

$$\gamma(\mathbf{k}) = \gamma_{\text{ph-ph}}(\mathbf{k}) + \gamma_{\text{sp-ph}}(\mathbf{k}). \quad (14)$$

For the damping due to the phonon–phonon interactions we have

$$\begin{aligned} \gamma_{\text{ph-ph}}(\mathbf{k}) = & \frac{3\pi}{N} \sum_q [B^2(\mathbf{q}, -\mathbf{k}, \mathbf{k} - \mathbf{q}) + B^2(\mathbf{q}, \mathbf{k} - \mathbf{q}, -\mathbf{q})] (\bar{N}_q - \bar{N}_{k-q}) \\ & \times [\delta(\omega_k - \omega_q - \omega_{k-q}) + \delta(\omega_k - \omega_q + \omega_{k-q})] \\ & + \frac{4\pi}{N^2} \sum_{q,p} A^2(\mathbf{q}, -\mathbf{k}, \mathbf{p}, \mathbf{k} - \mathbf{q} + \mathbf{p}) [\bar{N}_p (1 + \bar{N}_q + \bar{N}_{p+k-q}) - \bar{N}_q \bar{N}_{p+k-q}] \\ & \times \delta(\omega_k - \omega_q + \omega_p - \omega_{k+p-q}). \end{aligned} \quad (15)$$

$\gamma_{\text{sp-ph}}$ is the damping due to the spin–phonon interactions:

$$\begin{aligned} \gamma_{\text{sp-ph}}(\mathbf{k}) = & \frac{4\pi M^2}{N} \sum_q F_{\text{sp}}^2(\mathbf{q}, \mathbf{q} - \mathbf{k}) (\bar{m}_q - \bar{m}_{q-k}) \delta(E_{q-k} - E_q - \omega_k) \\ & + \frac{4\pi M^2}{N^2} \sum_{q,p} (R_{\text{sp}}^2(-\mathbf{k}, \mathbf{p}, \mathbf{q}) (\bar{m}_q - \bar{m}_p) [(1 + \bar{N}_{k+p-q}) \\ & \times \delta(E_p - E_q - \omega_{k+p-q} + \omega_k) + \bar{N}_{q-k-p} \delta(E_p - E_q + \omega_{q-k-p} + \omega_k)] \\ & + [R_{\text{sp}}^2(-\mathbf{k}, \mathbf{p}, \mathbf{q}) + R_{\text{sp}}^2(\mathbf{k} - \mathbf{q} + \mathbf{p}, \mathbf{p}, \mathbf{q})] \bar{m}_q (1 + \bar{m}_p) \\ & \times [\delta(E_p - E_q - \omega_{k+p-q} + \omega_k) - \delta(E_p - E_q + \omega_{q-k-p} + \omega_k)]) \\ & + \frac{\pi}{N^2} \sum_{q,p} [R_{\text{sp}}^2(-\mathbf{k}, \mathbf{p}, \mathbf{q}) + R_{\text{sp}}^2(\mathbf{k} - \mathbf{q} + \mathbf{p}, \mathbf{p}, \mathbf{q})] \langle S_p^z S_{-p}^z \rangle \langle S_q^z S_{-q}^z \rangle \\ & \times [\delta(E_p - E_q - \omega_{k+p-q} + \omega_k) - \delta(E_p - E_q + \omega_{q-k-p} + \omega_k)], \end{aligned} \quad (16)$$

where $\bar{N}_q = \langle a_q^\dagger a_q \rangle$ and $\bar{m}_q = \langle S_q^- S_q^\dagger \rangle$ are correlation functions which are calculated via the spectral theorem. At low temperatures the main contribution to the damping comes from the spin–phonon interaction, whereas in the vicinity of and above the phase transition temperature only the anharmonic phonon–phonon interaction terms remain.

The relative magnetization M is given for arbitrary spin value S by

$$M = \frac{1}{N} \sum_k [(S + 0.5) \coth[(S + 0.5)\beta E(\mathbf{k})] - 0.5 \coth(0.5\beta E(\mathbf{k}))], \quad (17)$$

where $E(\mathbf{k})$ is the renormalized spin-wave energy. It is calculated in the generalized Hartree–Fock approximation from the retarded Green’s function $g(\mathbf{k}, E) = \langle\langle S_{\mathbf{k}}^+; S_{\mathbf{k}}^- \rangle\rangle$ to:

$$\begin{aligned} E = & g\mu_B H + \frac{1}{2\langle S^z \rangle} \frac{1}{N} \sum_q (J_1^{\text{eff}}(q) - J_1^{\text{eff}}(k - q)) (2\langle S_q^z S_{-q}^z \rangle - \langle S_{k-q}^z S_{k-q}^\dagger \rangle) \\ & + \frac{1}{2\langle S^z \rangle} \frac{1}{N} \sum_q (J_2(q) - J_2(k - q)) (2\langle S_q^z S_{-q}^z \rangle - \langle S_{k-q}^z S_{k-q}^\dagger \rangle). \end{aligned} \quad (18)$$

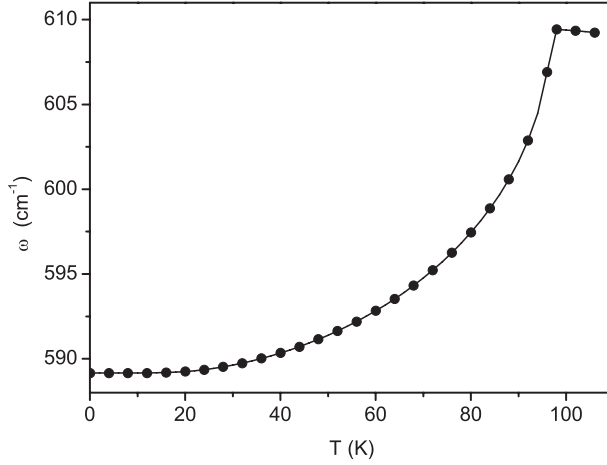


Figure 1. Temperature dependence of the phonon energy ω for $T = 40$ K and the following spin-phonon interaction constant: $R_{\text{sp}} = 10 \text{ cm}^{-1}$.

The spin exchange interaction constant between next-neighbours J_1 is renormalized due to the spin-phonon coupling to J_1^{eff} :

$$J_1^{\text{eff}} = J_1 + \frac{2F_{\text{sp}}^2}{\omega_0 + 0.5A - MR_{\text{sp}}}. \quad (19)$$

4. Numerical results and discussion

In this section we shall present the numerical calculations of our theoretical results taking the following model parameters which are appropriate for PrMnO_3 with $T_N = 97$ K: $J_1 = 108$ K, $J_2 = -60$ K, $A = -1 \text{ cm}^{-1}$, $B = 0.5 \text{ cm}^{-1}$, $F_{\text{sp}} = 10 \text{ cm}^{-1}$, $S = 2$. We have calculated the temperature dependence of the phonon energy for $\mathbf{k} = 0$ and different anharmonic spin-phonon interaction constants R_{sp} , which can be positive, $R_{\text{sp}} > 0$, or negative, $R_{\text{sp}} < 0$ [14]. The frequency shift below the phase transition temperature can be explained only if we assume a spin-dependent force constant given by the first and second derivatives of the exchange interaction $J_1(r_i - r_j)$ between the i th and j th ions with respect to the phonon displacements u_i, u_j . This displacement is interpreted by taking the nearest-neighbour exchange integral $J_1(r_i - r_j)$ and the next-nearest-neighbour exchange integral $J_2(r_i - r_j)$. The squared derivatives of J_1 and J_2 with respect to the phonon displacement can have opposite signs. This can be connected with the interaction and competition of the hybridized Mn d-states. There are both ferromagnetic and antiferromagnetic contributions that differ for in-plane and out-of-plane neighbours. But the competition between the exchange interaction of nearest- and next-nearest-neighbours is only one of the possible explanations. In principle, the different sign of R_{sp} can also be connected with different strains due to the influence of defects, ion doping, mechanical strain and with different ordering in the layers and between the layers in thin films etc.

The temperature dependence of the phonon energy for different spin-phonon interaction values is shown in figures 1 and 2. For positive R_{sp} values we obtain softening of the phonon mode with decreasing temperature, whereas for $R_{\text{sp}} < 0$ we have hardening of the phonon mode, i.e. the phonon energy is spin dependent. The obtained anomalous softening or hardening of the phonon modes is associated with the magnetic ordering. The demonstrated

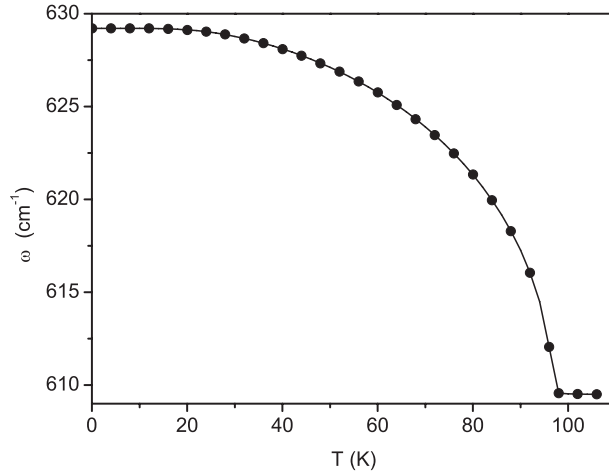


Figure 2. Temperature dependence of the phonon energy ω for $T = 40$ K and the following spin-phonon interaction constant: $R_{sp} = -10 \text{ cm}^{-1}$.

temperature behaviour of the phonon mode in the first case, $R_{sp} > 0$, is measured in the phonon spectra of RMnO_3 by Laverdiere *et al* [8], whereas the second case, $R_{sp} < 0$, could explain the hardening of the phonon energy observed in $\text{A}_2\text{Mn}_2\text{O}_7$ by Granado *et al* [13]. The exchange interactions in La-doped CaMnO_3 are studied using Raman scattering and electron paramagnetic resonance by Granado *et al* [16]. Dramatic reductions in the spin-phonon interactions and magnetic correlations are observed. All the modes broaden as the La concentration increases [16]. It can be seen from figures 1 and 2 that there is an anomaly, a kink around the magnetic phase transition temperature $T_N = 97$ K, which arises from the anharmonic spin-phonon interactions. The phonons show a magnetic shift below T_N , where the rare earth moments in RMnO_3 start to order. Above T_N , where only the anharmonic phonon-phonon interactions remain, the phonon energy slightly decreases.

The shift of the phonon spectra is dependent not only on the sign of the anharmonic spin-phonon interaction constant R_{sp} but also on the magnitude of R_{sp} (which is indirectly connected with the radius of the rare earth ion). This is demonstrated in figures 3 and 4. With increasing spin-phonon coupling R_{sp} the phonon frequency decreases linearly (figure 5). This is in accordance with the experimental data of Laverdiere *et al* [8]. They have shown that the sign and magnitude of the phonon shift appear to be correlated with the ionic radius of the rare earth ion r_R , evolving from softening for a larger radius to hardening for a smaller radius. Our spin-phonon interaction constant R_{sp} is connected through the first and second derivatives with the exchange interaction constant $J_1(r_i - r_j)$ which depends on the distance between the neighbouring spins. So it can be smaller when the distance is bigger, i.e. the radii of the ions are smaller, or greater for smaller distance, i.e. bigger radius. So we have different R_{sp} values in different compounds. Our theoretical results are in accordance with the experimentally obtained correlation of the phonon shift with the ionic radius of the rare earth ion. With decreasing R_{sp} , i.e. with decreasing radius of the rare earth ion r_R , the anomaly around T_N is smaller, for example for Y where the effect of magnetic ordering is much weaker. This is in agreement with the experimental data of Laverdiere *et al* [8] in RMnO_3 and those of Granado *et al* [13] in $\text{A}_2\text{Mn}_2\text{O}_7$. It is plausible to expect that the changes with r_R of the lattice distortions and magnetic structure will be reflected in changes of the phonon parameters and their variations near magnetic ordering temperature. The phonon energy shows a strong

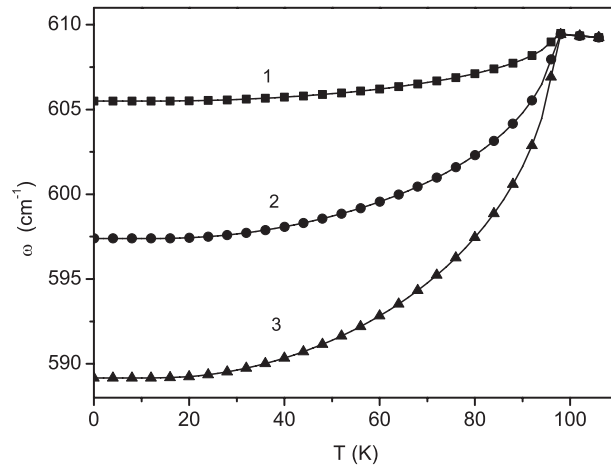


Figure 3. Temperature dependence of the phonon energy ω for $T = 40$ K and different spin-phonon interaction constants: (1) $R_{sp} = 2$, (2) 6 and (3) 10 cm^{-1} .

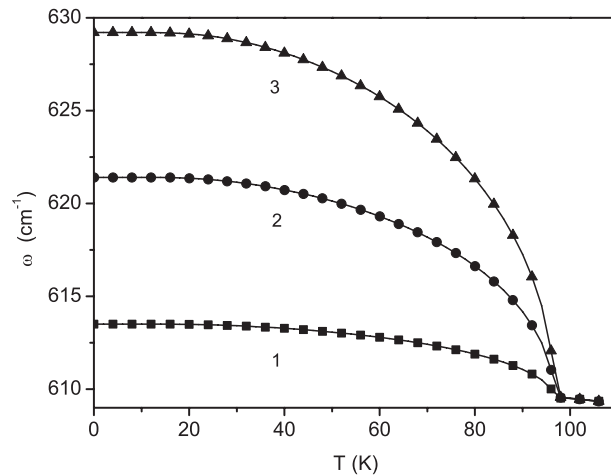


Figure 4. Temperature dependence of the phonon energy ω for $T = 40$ K and different spin-phonon interaction constants: (1) $R_{sp} = -2$, (2) -6 and (3) -10 cm^{-1} .

analogous dependence on the exchange interaction constant $J_1 (r_i - r_j)$, which depends on the distance between the spins and indirectly on the radius of the ions. ω decreases with increasing of J_1 (figure 6). It is evident from these results that frequency anomalies of the phonon modes may be expected as a consequence of magnetostrictive effects. Therefore, the anomalous softening or hardening shown in figures 1–4 may also be caused by a change in the lattice parameters at T_N . The magnetic phase transition temperature T_N decreases with decreasing exchange interaction J_1 (figure 7), i.e. with decreasing radius of the rare earth ion r_R . This is in accordance with the experimental data for RMnO_3 of Laverdiere *et al* [8] and Kimura *et al* [5]. They have observed that T_N decreases from 97 K for PrMnO_3 to 76 K for NdMnO_3 and 60 K for SmMnO_3 .

The phonon damping γ can be observed from the full width at half maximum in Raman spectroscopic experiments. We have calculated numerically γ in dependence on temperature

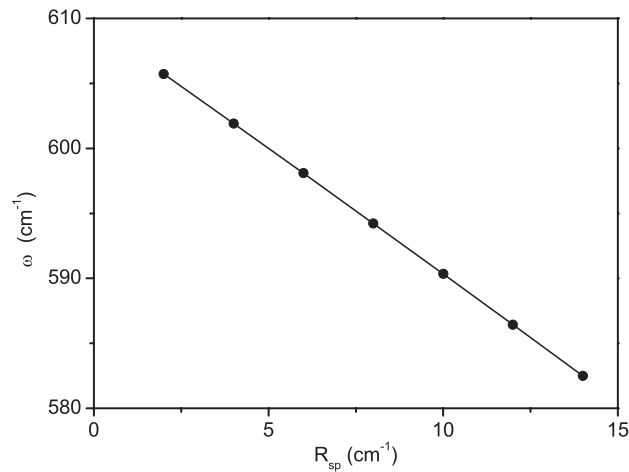


Figure 5. Dependence of the phonon energy ω on the anharmonic spin-phonon interaction constant R_{sp} for $T = 40$ K.

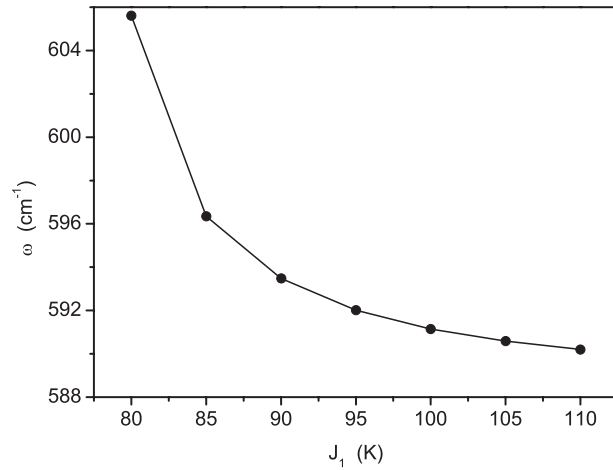


Figure 6. Dependence of the phonon energy ω on the exchange interaction constant J_1 for $R_{sp} = 10$ cm⁻¹ and $T = 40$ K.

and different interaction constants. The results are shown in figures 8 and 9. The damping increases with $T \rightarrow T_C$ (figure 8). It is clearly seen that around the phase transition temperature T_N there are strong anomalies, which is in agreement with the experimental data of Granado *et al* [9]. We obtain that the damping increases with R_{sp} (for the two cases $R_{sp} > 0$ and $R_{sp} < 0$, because the damping is proportional to R_{sp}^2). γ decreases with increase of the exchange interaction constants J_1 , too (figure 9). So, the phonon damping can be different for different exchange and spin-phonon interaction constants, i.e. different for substances with different ionic radii and doping concentrations. This is in accordance with the experimental data of Granado *et al* [9, 17], that the A_{1g} mode $R_{1-x}A_xMnO_3$ ($R = La, Pr$; $A = Ca, Sr$) is very sensitive to defects of the crystal lattice and that all modes broaden as the La concentration in $CaMnO_3$ increases.

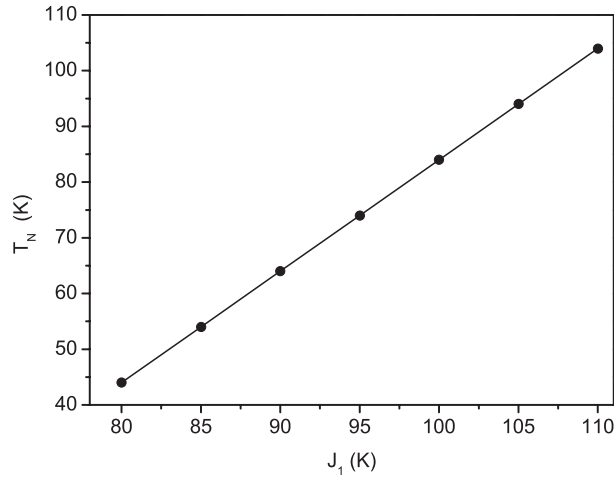


Figure 7. Dependence of the phase transition temperature T_N on the exchange interaction constant J_1 for $R_{sp} = 10 \text{ cm}^{-1}$.

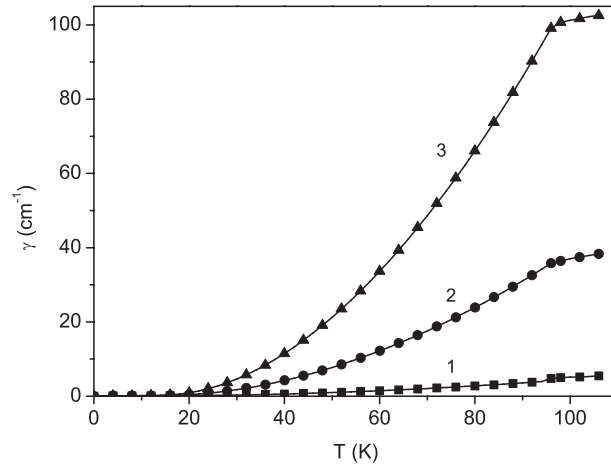


Figure 8. Temperature dependence of the phonon damping γ for different values of the magnetic spin-phonon interaction constant R_{sp} : (1) $R_{sp} = 2$, (2) 6 and (3) 10 cm^{-1} .

The discussion above was made for $H = 0$. The influence of an applied magnetic field H on the phonon energy can be seen in figures 10 and 11. The phonon energy ω can increase or decrease with increasing H in dependence of the sign of the anharmonic spin-phonon interaction constant. ω is enhanced for large magnetic fields for $R_{sp} < 0$ and reduced for the opposite case, $R_{sp} > 0$. The phonon damping always decreases for the two cases of R_{sp} with increasing applied magnetic field H (figure 12).

5. Conclusions

We have calculated the phonon spectrum in A-type manganites taking into account anharmonic spin-phonon and phonon-phonon interaction terms. We have obtained for the first time the temperature dependence of the phonon spectrum including damping effects for different

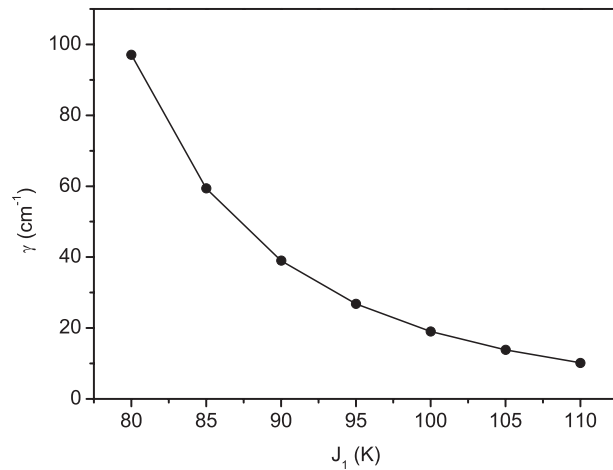


Figure 9. Dependence of the phonon damping γ on the exchange interaction constant J_1 for $R_{\text{sp}} = 10 \text{ cm}^{-1}$ and $T = 40 \text{ K}$.

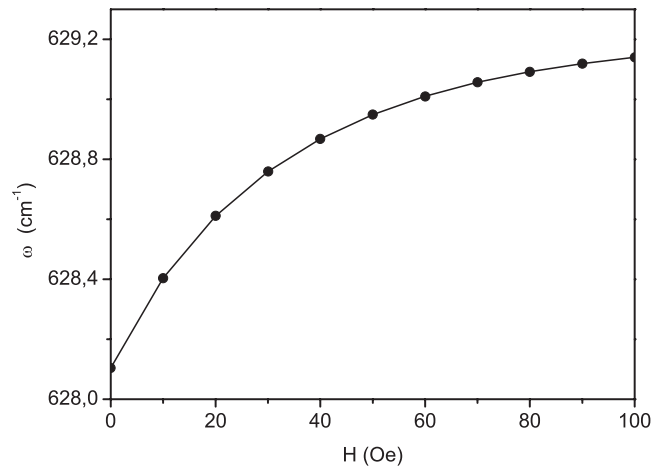


Figure 10. Dependence of the phonon energy ω on the magnetic field H for $R_{\text{sp}} = -10 \text{ cm}^{-1}$ and $T = 40 \text{ K}$.

exchange interaction J_1 and mostly for different spin–phonon interaction constants R_{sp} . In dependence of the sign of R_{sp} we obtain softening or hardening of the phonon modes with decreasing temperature below the phase transition temperature T_N . This is associated with the magnetic ordering below T_N and lattice anomalies caused by phonon modulation of the exchange integral. Therefore, the phonon–phonon interactions cannot explain the observed shift of the phonon modes. We suggest that the anharmonic spin–phonon interaction is responsible for the anomalous behaviour of ω in the orthorhombic manganites RMnO_3 and the manganese-based compounds $\text{A}_2\text{Mn}_2\text{O}_7$. The phonon energy and the phonon damping show strong anomalies around the phase transition temperature T_N which are due to the spin–phonon interaction. With decrease in the spin–phonon coupling R_{sp} , i.e. decreasing radius of the rare earth ion, the phonon frequency shifts towards higher values and the anomaly around T_N is smaller, for example for Y where the effect of magnetic ordering is much weaker. This

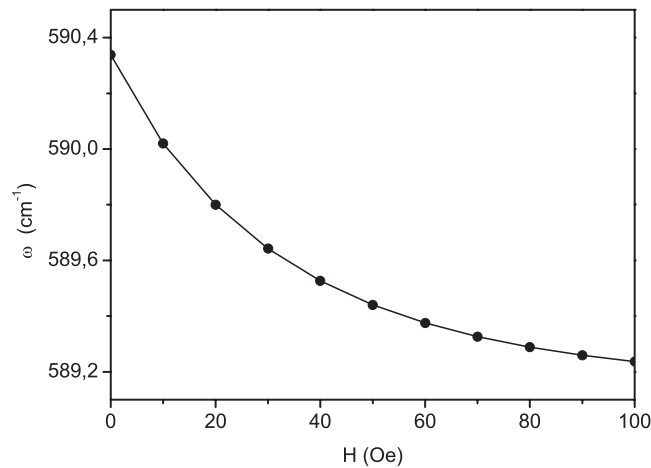


Figure 11. Dependence of the phonon energy ω on the magnetic field H for $R_{sp} = 10 \text{ cm}^{-1}$ and $T = 40 \text{ K}$.

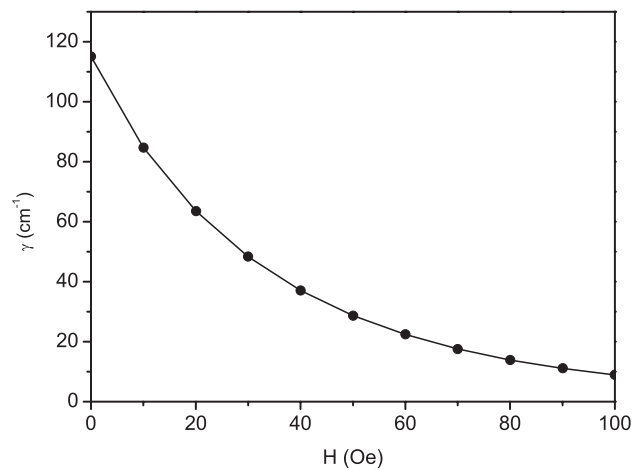


Figure 12. Dependence of the phonon damping γ on the magnetic field H for $R_{sp} = -10 \text{ cm}^{-1}$ and $T = 40 \text{ K}$.

is in agreement with the experimental data of Laverdiere *et al* [8] in RMnO_3 and those of Granado *et al* [13] in $\text{A}_2\text{Mn}_2\text{O}_7$. We obtain that the phonon damping is strongly dependent on the exchange interaction constants J_1 , and on the spin–phonon interaction constants R_{sp} . It can be very different in dependence on these interaction constants which are different for different substances. So we could explain the different line widths of the experimental data of Granado *et al* [9, 17]. The influence of an external magnetic field is discussed, too. The phonon energy ω can be enhanced for large magnetic fields for $R_{sp} < 0$ and reduced for the opposite case, $R_{sp} > 0$. The phonon damping γ always decreases with increasing magnetic field H .

References

- [1] Smolenskij G A and Chupis I E 1982 *Sov. Phys.—Usp.* **25** 475
- [2] Lorenz B, Wang Y Q, Sun Y Y and Chu C W 2004 *Phys. Rev. B* **70** 212412

- [3] von Helmolt R, Wecker J, Holzapfel B, Schultz L and Samwer K 1993 *Phys. Rev. Lett.* **71** 2331
- [4] Jin S, Tiefel T H, McCormack M, Fastnacht R A, Ramesh R and Chen L H 1994 *Science* **64** 413
- [5] Kimura T, Ishihara S, Shintani H, Arima T, Takahashi K T, Ishizaka K and Tokura Y 2003 *Phys. Rev. B* **68** 060403(R)
- [6] Goto T, Kimura T, Lawes G, Ramirez A P and Tokura Y 2004 *Phys. Rev. Lett.* **92** 257201
- [7] Iliiev M N, Abrashev M V, Laverdiere J, Jandl S, Gospodinov M M, Wang Y-Q and Sun Y-Y 2006 *Phys. Rev. B* **73** 064302
- [8] Laverdiere J, Jandl S, Mukhin A A, Ivanov V Yu, Ivanov V G and Iliiev M N 2006 *Phys. Rev. B* **73** 214301
- [9] Granado E, Moreno N O, Garcia A, Sanjurjo J A, Rettori C, Torriani I, Oseroff S B, Neumeier J J, McClellan K, Cheong S W and Tokura Y 1998 *Phys. Rev. B* **58** 11435
- [10] Granado E, Garcia A, Sanjurjo J A, Rettori C, Torriani I, Prado F, Sanchez R, Caneiro A and Oseroff S B 2004 *Phys. Rev. B* **60** 11879
- [11] Iliiev M N and Abrashev M V 2001 *J. Raman Spectrosc.* **32** 805
- [12] Jandl S, Barilo S N, Shiryaev S V, Mukhin A A, Ivanov V Yu and Balbashov A M 2003 *J. Magn. Magn. Mater.* **264** 36
- [13] Granado E, Pagliuso P G, Sanjurjo J A, Rettori C, Subramanian M A, Cheong S-W and Oseroff S B 1999 *Phys. Rev. B* **60** 6513
- [14] Wesselinowa J M 1986 *J. Phys. C: Solid State Phys.* **19** 6973
Wesselinowa J M 1991 *J. Phys.: Condens. Matter* **3** 5231
- [15] Wesselinowa J M and Apostolov A T 1996 *J. Phys.: Condens. Matter* **8** 473–88
- [16] Tserkovnikov Yu A 1971 *Teor. Mat. Fiz.* **7** 250
- [17] Granado E, Moreno N O, Martinho H, Garcia A, Sanjurjo J A, Torriani I, Rettori C, Neumeier J J and Oseroff S B 2001 *Phys. Rev. Lett.* **86** 5385